Improving the Ionic Conductivity of Carboxylated Nitrile Rubber/LDH Composites by Adding Imidazolium Bis(trifluoromethylsulfonyl)imide Ionic Liquids

Anna Laskowska,*[1] *Anna Marzec*,[1] *Gisele Boiteux*,[2] *Marian Zaborski*,[1] *Olivier Gain*,[2] *Anatoli Serghei*,[2] *Waldemar Maniukiewicz*[3]

Summary: We investigated the ability of three imidazolium ionic liquids (ILs) (1-ethyl-3-methylimidazolium bis(trifluoromethylsulfonyl)imide (EMIM TFSI), 1-butyl-3-methylimidazolium bis(trifluoromethylsulfonyl)imide (BMIM TFSI), 1-hexyl-methylimidazolium bis(trifluoromethylsulfonyl)imide (HMIM TFSI)) that have the same anion but different alkyl chain lengths of cation in amounts of 2.5, 5, 10 and 15 phr (parts per hundred rubber)to improve the ionic conductivity of carboxylated nitrile butadiene rubber (XNBR)/layered double hydroxide (MgAl-LDH) composites. The presence of these ionic liquids modified the relaxation behavior of the XNBR matrix. Increasing the length of the cation side-chain (from ethyl- to hexyl-) impactsthe glass transition temperature of the rubber matrix, the crosslink density, the mechanical properties and the ionic conductivity of the resulting XNBR/IL-LDH composites. Among this group of ionic liquids, 1-ethyl-3-methylimidazolium bis(trifluoromethylsulfonyl)imide (EMIM TFSI)or alternatively 1-butyl-3-methylimidazolium bis(trifluoromethylsulfonyl)imide (BMIM TFSI)proved most suitable for enhancingthe ionic conductivity of rubber composites without substantial deterioration of their mechanical properties.

Keywords: carboxylated nitrile rubber; composites; dielectric properties; elastomers; ionic liquids

Introduction

Ionic liquids (ILs) are organic salts composed entirely of ions, and most are liquids at room temperature.[1] Many recent publications have demonstrated that ILs play an increasingly important role in the preparation of functional elastomer materials. Given their low vapor pressure, nonflammability, high chemical and thermal stability, ILs may serve multiple functions in the preparation of elastomer composites and have been already recognized as processing aids for the melt processing of rubber/filler composites,[2] plasticizers that reduce the glass transition temperature of an elastomer matrix,[3] interfacial modifiers (compatibilizers for improving filler dispersion)[4] and cure accelerators.[5] In addition, ILs can act as ion reservoirsto increase the ionic conductivity of polymer composites.[6] Doping rubbers with ionic liquids is a simple way to change their critical properties including mechanical, thermal and antimicrobial and to prepare composites with high ionic conductivity and good

[1] Institute of Polymer and Dye Technology, Technical University of Lodz, Stefanowskiego 12/16, 90924 Lodz, Poland
Fax: (+48) 426362543;
E-mail: anna.laskowska@hotmail.com
[2] Ingénierie des Matériaux Polymères, Université Claude Bernard Lyon1, UMR CNRS 5223, 15 Bd A.Latarjet, 69622 Villeurbanne, France
[3] Institute of General and Ecological Chemistry, Technical University of Lodz, Zeromskiego 116, 90924 Lodz, Poland

elasticity. High ionic conductivity enables ILs to play an important role in enhancing polymer conductivity.ILs based on the bis(trifluoromethylsulfonyl)imide anion ($TFSI^-$) are suitable for a wide range of electrochemical applications (supercapacitors, sensors, biosensors) due to their high conductivity and high electrochemical stability. Generally, ionic liquids have excellent ionic conductivity up to their decomposition temperature. Unlike other highly conductive but much less electrochemically and thermally stable ILs(e.g., those containing dicyanamide ($N(CN)_2$) or thiocyanate (SCN) ions), TFSI-based imidazolium salts are characterized by high chemical and thermal stability up to 380 °C.[7] The thermal stability of ILs is a critical factor in their suitability at the high temperaturesinvolved in the melt-blending process.Hydrophobicity (immiscibility with water)[1] is another advantage of TFSI-based imidazolium ILs making them more compatible with hydrophobic rubber matrices, preventing leakage (migration within the polymer matrix), facilitating rubber processing and improving filler dispersion throughout the elastomer matrix. Additionally, the immiscibility with water increases with increasing length of the cation side chain due to the increased surface activity of longer-chain cations.[8] The use of TFSI-based imidazolium ILs as processing aids, filler-matrix compatibilizers (interfacial modifiers) and conductivity enhancers in elastomers has been already reported for hydrogenated nitrile rubber (HNBR),[9] chloroprene rubber (CR),[10–15] nitrile rubber (NBR)[6,16–19] and solution styrene butadiene rubber (SSBR).[20] Most publications present the ability of IL-modified carbon nanotubes (CNTs) or carbon black (CB)[21] to improve rubber conductivity and filler dispersion. Few studies have investigated the ability of substances containinghigh levels of pure ionic liquids to improve the ionic conductivity of rubber materials[6,16–19] (e.g.,Marwanta et al. prepared a conductive rubber material based on a nitrile elastomer (NBR) and an ionic liquid).[6,17] In addition, no information is available regarding the effect of the imidazolium salt cation structure on the ionic conductivity and other properties of elastomer composites (e.g., crosslink density, mechanical propertiesand glass transition temperature of the rubber matrix). We report the results of our studies on the cure, mechano-dynamical properties and ionic conductivity of rubber composites based on carboxylated nitrile rubber/layered double hydroxide and hydrophobic ionic liquids with the same anion bis(trifluoromethylsulfonyl)imide with backbone lengths of imidazolium cation ring that vary from ethyl to hexyl. Systems such as XNBR/LDH are based on ionic/polar interactions and yield transparent, ionic elastomer materials when crosslinks form due to the acid-base interactions between the carboxylic groups of the XNBR and the LDH filler.

Experimental Part

Materials

The carboxylated acrylonitrile-butadiene rubber XNBR used in this study was Krynac X 750 (7 wt% carboxyl groups, 27 wt% acrylonitrile, Mooney viscosity (ML1 + 4(100 °C):47)) supplied by Lanxess (Germany). Magnesium aluminum layered double hydroxide MgAl-LDH, designated here as LDH (Sigma Aldrich, Germany), served asboth a filler and a curing agent in the XNBR compounds. The ionic liquids 1-ethyl-3-methylimidazolium bis(trifluoromethylsulfonyl) imide (EMIM TFSI), 1-butyl-3-methylimidazolium bis(trifluoromethylsulfonyl) imide (BMIM TFSI) and 1-hexyl-3-methylimidazolium bis(trifluoromethylsulfonyl) imide (HMIM TFSI) (designated here as the general alkyl-MIM TFSI) were supplied by Sigma Aldrich (Germany).

Preparation of the Composites

The LDH (30 parts per hundred rubber (phr)) was combined with varyingquantities (2.5, 5, 10 and 15 phr) of alkyl-MIM TFSI by grinding it until a homogeneous paste was obtained. The rubber compounds were

processed in an internal Brabender N50 measuring mixer at 40 rpm rotor speed and an initial temperature of 60 °C. After approximately 5 minutes of rubber mastication, the mixture composed of the LDH filler and IL was added and homogenized for around 10 minutes. Then, the compounded rubbers were milled in a laboratory two-roll mill (friction ratio 1:1.2, roll temperature = 40 °C, dimensions: diameter = 200 mm, length = 450 mm). The cure characteristics of the XNBR/IL-LDH composites were determined using a moving die rheometer (M < PREFIX > DR </PREFIX > 3000, MonTech, Germany) at 160 °C for 120 minutes. A sinusoidal strain of 7% and frequency of 1.67 Hz were applied. The optimum cure time (t_{90}), scorch time (t_2), minimum torque (ML), maximum torque (MH) and delta torque (ΔM) were determined from the curing curves. The mixed stocks were cured in a standard hot press at 160 °C, for the $t_{90}$of the respective samples. The rubber sheets obtained from thus had a thickness below 1 mm.

Testing and Characterization

The crosslink density within the vulcanized network was determined via equilibrium swelling. The vulcanizates were subjected to equilibrium swelling in toluene for 48 h at room temperature. The swollen samples were then weighted on a torsion balance, dried to a constant weight in a dryer at 60 °C and reweighed after 48 h. The crosslinking density was determined based on Flory-Rehner's equation.[22] Stress-strain tests were performed on a universal material testing machine (Zwick model 1435) with a crosshead speed of 500 mm/minaccording to the standard PN-ISO 37-2007. To measure the tensile properties, five dumbbell-shaped specimens were punched from each rubber sample and the average value of each formulation was reported. The stress at break, modulus at 100%, 200% and 300% elongation and the elongation at break were measured at room temperature. Differential scanning calorimetry (DSC) measurements (Q 200 DSC, TA Instrument, USA) of the samples were performed at a heating rate of 10 °C min^{-1} in the temperature range from -80 to 180 °C under a nitrogen atmosphere. The glass transition temperatures (T_g) were determined at the midpoint of the step. Dielectric measurements were conducted via broadband dielectric spectroscopy (BDS) (Novocontrol alpha analyzer, Hundsagen, Germany) in the frequency range from 10^{-1} to 10^7 Hz at room temperature. The samples were placed between two copper electrodes with diameters of 20 mm. Dynamic mechanical analysis (DMA) of composites was performed using a dynamic mechanical analyzer (Q 800 DMA, TA Instruments, USA). The storage modulus (E'), loss modulus (E″) and loss tangent (tan δ) were measured in the tension mode within the temperature range from -90 to 100 °C at a frequency of 10 Hz and a heating rate of 2 °C/min. Thermogravimetric analysis (Q 500 TGA, TA Instruments, USA) was performed in the temperature range from 50 to 600 °C under a helium atmosphere at a heating rate of 10 °C/min. The morphology of the elastomer matrices was observed via SEM with a LEO 1530 SEM microscope. The rubber composites were broken down in liquid nitrogen, and the fractured surfaces of the vulcanizates were examined. Room-temperature powder X-ray diffraction patterns were collected using a PANalyticalX'Pert Pro MPD diffractometer in Bragg-Brentano reflecting geometry with(CuKα) radiation from a sealed tube. Data were collected in the 2θrange of 2–70° with a 0.0167° step and 20-s exposition per step.

Results and Discussion

Cure Characteristics, Crosslink Density and Mechanical Properties

The effects of increasing the alkyl chain length of the imidazolium ring from ethyl to hexyl and the increasing the IL quantity from 2.5 to 15 phr were investigated with regards to the curing behavior, crosslink density and stress-strain behavior of the XNBR/LDH. The rheometric parameters of the rubber mixes are provided in Table 1,

Table 1.
Rheometric characteristics of XNBR/IL-LDH composites crosslinked at 160 °C.

ILtype and content	ML[a)]	MH[b)]	ΔM[c)]	t_2[d)]	t_{90}[e)]	CRI[f)]
phr	dNm	dNm	dNm	min	min	min^{-1}
–	1.4	6.6	5.2	4.1	77	1.37
EMIM TFSI 2.5	1.1	5.3	4.2	2.4	63	1.68
EMIM TFSI 5	1.2	5.0	3.8	2.5	62	1.77
EMIM TFSI 10	1.0	4.6	3.6	3.2	62	1.67
EMIM TFSI 15	1.0	5.2	4.2	3.3	61	1.69
BMIM TFSI 2.5	1.2	5.4	4.2	2.5	65	1.60
BMIM TFSI 5	1.1	5.3	4.2	2.6	63	1.65
BMIM TSFI 10	1.1	4.8	3.7	3.2	64	1.64
BMIM TSFI 15	0.8	4.0	3.2	3.8	63	1.69
HMIM TFSI 2.5	1.1	5.3	4.2	2.0	58	1.78
HMIM TFSI 5	1.1	4.9	3.8	2.5	56	1.90
HMIM TFSI 10	0.8	4.3	3.5	3.4	65	1.62
HMIM TFSI 15	0.7	3.9	3.2	3.9	66	1.61

[a)] Min. torque.
[b)] Max. torque.
[c)] Difference between maximum torque and minimal torque, torque increment.
[d)] Scorch time.
[e)] Optimal curing time.
[f)] Cure rate index.

which indicates that such ILs with $TFSI^-$ anionsslightly accelerate the curing process of XNBR by LDH. The optimal cure time (t_{90}) is reduced when a small quantity (2.5 phr) of IL is added and remained almost unchanged regardless of the alkyl side length and the IL content. From the rheometric data we can also observe changes in the minimum torque (ML), which reflects the viscosity of the rubber mix, and the torque increment (ΔM), which is a good indicator of crosslink formation.

Increasing the alkyl chain length of imidazolium cation from ethyl to hexyl decreases the mix viscosity and hinders network formation,whichare reflected in reduced ML and ΔM values in comparison with the reference sample. Numerous studies have determined that ionic liquids containing $TFSI^-$ ions act as plasticizers in rubber compounds.[6,9,16–19] In the current study, the plasticizing effect of 1-hexyl-3-methylimidazolium was found to be the highest likely due to its bulky structure. The mechanism for crosslinking XNBR with magnesium aluminum layered double hydroxides MgAl-LDHs is based on the neutralization of acidic carboxylic groups -COOH (only 7 wt% carboxyl functionalities) by the basic hydroxyl groups presenton the LDH surface, additionally MgAl-LDH filler may provide the metal ions for metal-carboxylate curing.[23–26] In such systems, a rubber material is substantially reinforced by the strong chemical interactions (polar/ionic) between the carboxylic rubber and the LDH filler rendering the addition of standard curatives unnecessary. Moreover, the crosslinking of XNBR with MgAl-LDH yields transparent properties in the final composite, even in the presence of 30 phr of mineral. The incorporation of TFSI-based IL at loadings 2.5–10 phr had no significant effect on the XNBR/LDH optical properties, however the presence of IL at higher concentration contributed to obtain a cloudy (milky) color material. The mechanical parameters of the control and samples containing IL are presented in Table 2 and Figure 1.

The incorporation of small quantities (2.5 or 5 phr) of TFSI-based IL with an ethyl side chain attached to the imidazolium ring results in a slight increase in the tensile strength (TS) and elongation at break (EB) of the XNBR/IL-LDH composite, however increasing the quantity of EMIM TFSI to 10 or 15 phr decreases stress at break (TS) and yields a rubbermaterial of higher elasticity. The same trend is observed in

Table 2.
Mechanical properties ofXNBR/IL-LDH composites.

ILtype and content	SE_{100} [a]	SE_{200} [b]	SE_{300} [c]	TS[d]	EB[e]	Shore A Hardness
phr	MPa	MPa	MPa	MPa	%	°Sh
–	3.0 ± 0.1	5.3 ± 0.1	6.3 ± 0.1	17.6 ± 2.0	634 ± 20	62
EMIM TFSI 2.5	2.6 ± 0.1	4.4 ± 0.1	5.9 ± 0.1	19.4 ± 0.5	665 ± 20	62
EMIM TFSI 5	2.5 ± 0.1	4.3 ± 0.1	5.9 ± 0.1	18.8 ± 0.5	677 ± 10	62
EMIM TFSI 10	2.2 ± 0.1	3.7 ± 0.1	5.1 ± 0.1	16.8 ± 0.5	678 ± 30	61
EMIM TFSI 15	1.9 ± 0.1	3.3 ± 0.1	4.6 ± 0.1	14.1 ± 0.5	694 ± 20	59
BMIM TFSI 2.5	2.3 ± 0.1	4.0 ± 0.2	5.5 ± 0.2	18.2 ± 1.0	682 ± 10	63
BMIM TFSI 5	2.2 ± 0.1	3.8 ± 0.1	5.2 ± 0.1	18.0 ± 0.5	685 ± 20	62
BMIM TSFI 10	2.2 ± 0.2	3.7 ± 0.3	5.1 ± 0.5	17.5 ± 0.8	690 ± 20	62
BMIM TSFI 15	1.7 ± 0.1	2.8 ± 0.1	3.9 ± 0.1	13.4 ± 0.5	727 ± 20	59
HMIM TFSI 2.5	2.1 ± 0.1	3.5 ± 0.1	4.7 ± 0.1	15.0 ± 1.0	717 ± 20	61
HMIM TFSI 5	2.1 ± 0.1	3.5 ± 0.1	4.8 ± 0.1	15.1 ± 1.0	719 ± 20	60
HMIM TFSI 10	2.0 ± 0.1	3.5 ± 0.1	4.8 ± 0.1	14.7 ± 1.0	725 ± 20	59
HMIM TFSI 15	1.7 ± 0.1	2.8 ± 0.1	3.9 ± 0.1	13.5 ± 1.0	741 ± 20	58

[a] Stress modulus at 100% elongation.
[b] Stress modulus at 200% elongation.
[c] Stress modulus at 300% elongation.
[d] Tensile strength.
[e] Elongation at break.

the mechanical parameters when the IL content increasedfor BMIM TFSI and HMIM TFSI. The presence of HMIM TFSI had the greatest impact in increasingthe elongation at break (EB) and decreasingthe tensile strength (TS) of the XNBR/LDH composite. The plasticizing effect from extending the alkyl chain lengthon the imidazolium ring is obvious even at the low concentration of 2.5 phr in the rubber matrix.

The performance characteristics of the rubber materials are maintained despite the presence of a high quantity of IL, which in excess acts as a plasticizer in the composite. Additionally, the reduced tensile strength (TS) and increased elongation at break (EB) in the presence of high IL levels in the XNBR/LDH compound result from the lowered crosslink density of the composite. We assume that a thinlayer of IL present onto the filler particle surfacesmay hinderboth the filler-rubber interactions and the formation of ionic crosslinks. The detrimental effect of the TFSI ionic liquids on the rubber network formation in the XNBR/LDH composite was evidenced by equilibrium swelling measurements in toluene. Results from this experiment are presented in Figure 2, which indicates that the decreased crosslink density is a result of the increased IL concentration and the longer alkyl side chain on the imidazolium ring. Compared with BMIM TFSI and HMIM TFSI, the use of EMIM TFSI is more preferable considering mechanical characteristics of the resulting composites.

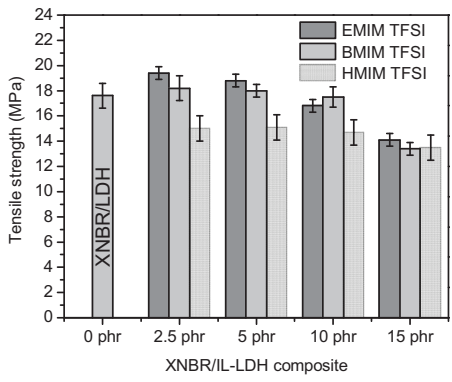

Figure 1.
Effect of ILs type and loading on tensile strength of XNBR/LDH composites.

Effect of ILs on the Glass Transition Temperature (T_g) and Dynamic Mechanical Properties

Dynamic mechanical analysis (DMA) was performed on the reference sample and

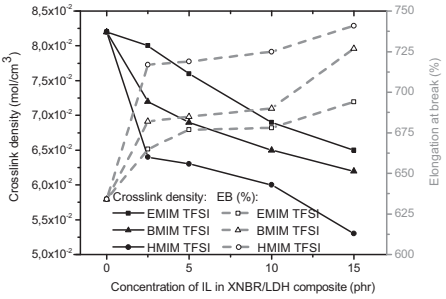

Figure 2.
Effects of ILs type and loading on crosslink density andelongation at break of XNBR/LDH composites.

composites containing 15 phr IL at a vibration frequency of 10 Hz. The loss tangent (tan δ), storage modulus (E')and loss modulus (E″)as functions of temperature are illustrated in Figure 3a–d. The glass transition temperatures (T_g) were measured via DSC and DMA and are reported in Table 3.

Both methods exhibited a single T_g for all composites suggesting no microphase separation. However, when measuring the T_g of rubber materials, DMA appears more sensitive, providing more precise values than DSC. The incorporation of 15 phr TFSI-based ILs into the XNBR matrix substantially altered the T_g (Table 3) in each case. Increasing the length of the alkyl backbone of the imidazolium ring caused a decrease in T_g (DSC) from -31 °C for the EMIM TFSI sample to -33 °C for the BMIM and HMIM TFSIs. The plasticizing effect of the TFSI-based ILs on various rubber matrices has previously been reported in the literature.[6,9,16–19] Figure 3a demonstrates that the loss tangent (tan δ) of the XNBR/LDH composites presents two relaxations. The low temperature relaxation corresponds to the glass transition temperature (T_g) of the composite. The other relaxation in the temperature range from 20 to 80°C with a maximum at around 50°C is the so-called ionic transition temperature T_i and indicates the existence of ionic crosslinks formed whenthe XNBR is crosslinked by

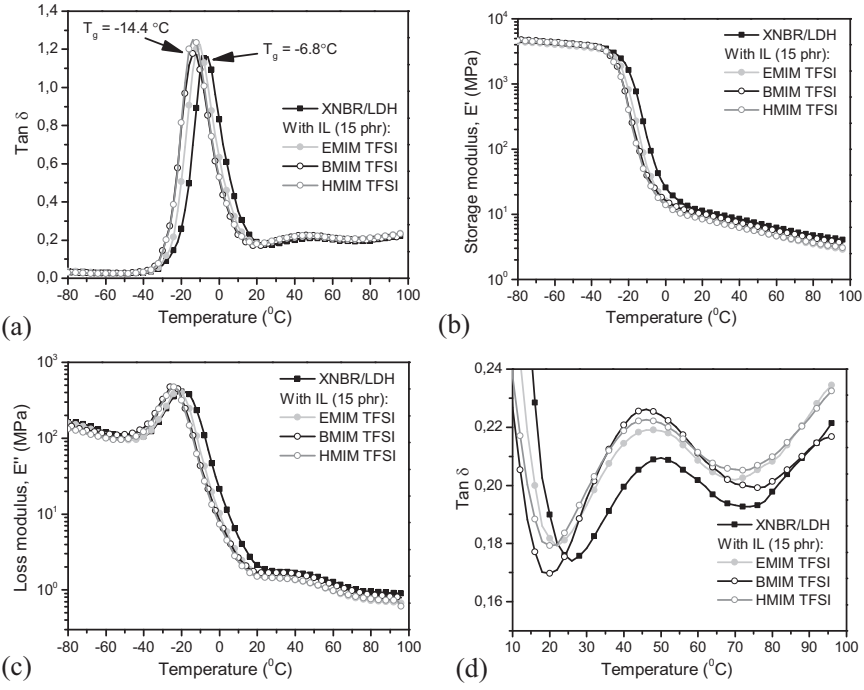

Figure 3.
(a) Plot of tan δ, (b) plot of storage modulusE' (c) plot of loss modulus E″versus temperature (d) ionic transition region of XNBR/LDH composites containing 15 phr of IL.

Table 3.
Glass transition temperature (T_g) derived from DSC and DMA and storage modulus (E') DMA at 10 Hz.

ILtype and content	T_g (DSC)	T_g from E″	T_g from tan δ	Height of tan δ max	E' at 25 °C
phr	°C	°C	°C	–	MPa
–	−23	−17.1	−6.8	1.2	10.4
EMIM TFSI15	−31	−22.0	−10.9	1.2	8.0
BMIM TFSI 15	−33	−24.4	−14.4	1.2	7.9
HMIM TFSI15	−33	−24.9	−14.4	1.3	7.8

the magnesium-aluminum layered double hydroxides LDH.Such clusters melt at higher temperaturescausing an additional tan δ peak during DMA analysis (Figure 3d).

We may observe that the TFSI-based IL at 15 phr of concentration changed the height and position of T_i peak of the XNBR/LDH composite, which is higher and shifted towards lower temperatures in comparison to the control sample. This transition (ionic transition) takes place in a wide range of temperatures and includes, not only the ionic transition, but also the softening of the material.[27] Analyzing the plots form Figure 3d, we make an assumption that the presence of IL in XNBR/LDH composite softened the hard phase arising from the interactions between XNBR and MgAl-LDH.The tan δ peak maximumis also shifted towards lower temperatures form -6.8 (control) to −10.9 °C (15 phr EMIM TFSI) and approximately −14.4 °C (15 phr BMIM TFSI and 15 phr HMIM TFSI). The changes in T_g in the XNBR/IL-LDH composites depend slightly on the alkyl backbone length in the imidazolium ring of the incorporated IL, however the greatest plasticization was detected in sample containing the HMIM TFSI ionic liquid.

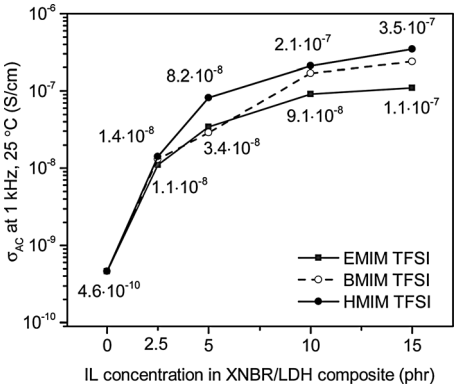

Figure 4.
AC conductivity in function of IL type and amount in XNBR/IL-LDH composites.

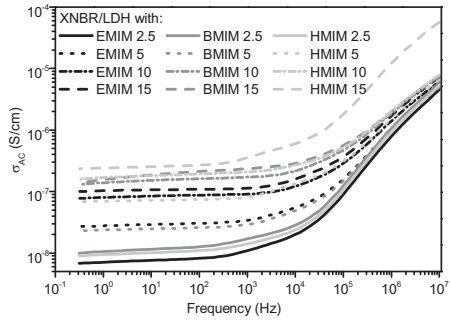

Figure 5.
AC conductivity of XNBR/LDH composites versus frequency, measured at room temperature.

Increased Ionic Conductivity of the XNBR/IL-LDH Composites

The increased level of the ionic liquid in the polymer causes an increase in the ionic conductivity of the composite. However, the improved conductivity of the rubber materials is a function not only of the number of IL ions but also the plasticizing effect of the ILs on the rubber matrix.

The current work (Table 4) confirmed the relationship between the plasticization effect and the increased conductivity of the polymer/IL material. As indicated in Table 4, the decrease in T_g with increasing TFSI-based IL content enhanced the mobility and increased the ionic conductivity. The increased ionic conductivity of the composite can be largely attributed to the

Table 4.
Effects of ILs on glass transition temperature (T_g) and AC conductivity (σ_{AC}) of XNBR/IL-LDH composites (σ_{AC} measured at room temperature).

IL type and content	T_g (DSC)	ΔT_g	σ_{AC}, 1 Hz	σ_{AC}, 1 kHz
phr	°C	°C	$S \cdot cm^{-1}$	$S \cdot cm^{-1}$
–	−23	–	$1.4 \cdot 10^{-10}$	$4.6 \cdot 10^{-10}$
EMIM TFSI 2.5	−24	1	$7.1 \cdot 10^{-9}$	$1.1 \cdot 10^{-8}$
EMIM TFSI 5	−26	3	$2.8 \cdot 10^{-8}$	$3.4 \cdot 10^{-8}$
EMIM TFSI 10	−28	5	$8.0 \cdot 10^{-8}$	$9.1 \cdot 10^{-8}$
EMIM TFSI 15	−31	8	$1.0 \cdot 10^{-7}$	$1.1 \cdot 10^{-7}$
BMIM TFSI 2.5	−24	1	$1.1 \cdot 10^{-8}$	$1.3 \cdot 10^{-8}$
BMIM TFSI 5	−26	3	$2.5 \cdot 10^{-8}$	$2.9 \cdot 10^{-8}$
BMIM TSFI 10	−28	5	$1.2 \cdot 10^{-7}$	$1.7 \cdot 10^{-7}$
BMIM TSFI 15	−33	10	$1.6 \cdot 10^{-7}$	$2.4 \cdot 10^{-7}$
HMIM TFSI 2.5	−24	1	$9.4 \cdot 10^{-9}$	$1.4 \cdot 10^{-8}$
HMIM TFSI 5	−26	3	$7.0 \cdot 10^{-8}$	$8.2 \cdot 10^{-8}$
HMIM TFSI 10	−29	6	$1.3 \cdot 10^{-7}$	$2.1 \cdot 10^{-7}$
HMIM TFSI 15	−33	10	$1.7 \cdot 10^{-7}$	$3.5 \cdot 10^{-7}$

increased motion of the rubber chain segmentsin the XNBR/IL-LDH. In addition, the TFSI-based IL acts a reservoir of effective carrier ions and their increasing concentration in the composite contributes to the higher observed values of σ_{AC}.

Considering the effect of the IL quantity, the sharpest increase in the AC conductivity of a rubber material was observed when 2.5 or 5 phr IL was added, further increases in the IL content resulted in smoother changes in the σ_{AC} for the composites. It seems that theAC conductivity is much more depended on the TFSI-based IL concentration than ontheincrease in the length of the alkyl backbone of the imidazolium ring. The most significant change in $\sigma_{AC}$was reported for the XNBR/LDH sample containing the highest amount of 1-hexyl-3-methylimidazolium TFSI salt. Thedifferences in σ_{AC}values of the samplescontaining EMIM, BMIMand HMIM TFSI at corresponding concentrations are less significant than anticipated.

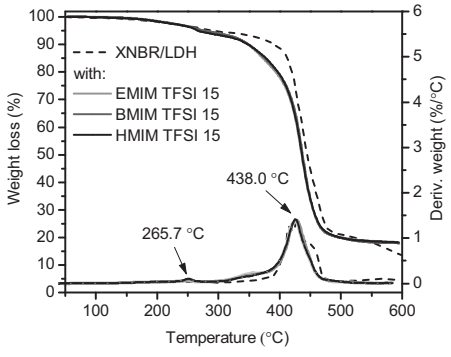

Figure 6.
TGA/DTG curves of XNBR/LDH composites containing 15 phr of TFSI-based IL.

Effect of ILs on the Thermal Stability

The thermal stability of the XNBR/LDH composites containing 15 phr TFSI-based ILs was analyzed via thermogravimetric analysis (TGA). The TGA curves of the rubber samples with TFSI-based IL exhibited no thermal changes below 252.6°C (Figure 6).

The addition of 15 phr IL increasedthe decomposition temperature at 2% mass loss (T_2) of XNBR/LDH. The ILs used as components in rubber composites should be characterized by sufficient thermal stability to allow them to withstand the high temperatures used during both the melt-blending and curing processes of the composites. The TFSI-based imidazolium ionic liquids satisfy this requirement. The decomposition temperature of the TFSI-based imidazolium ionic liquids is below that of the XNBR/LDH, therefore, the T_5, T_{10} and T_{50} shift toward lower temperatures is observed (Table 5).The observed higher thermal stability of XNBR/LDH/EMIM TFSI composite in

Table 5.
Thermal properties of XNBR/IL-LDH composites containing 15 phr of IL.

IL type	T_2	T_5	T_{10}	T_{50}	Char residue
	°C	°C	°C	°C	wt%
–	207	291	391	445	13.45
EMIM TFSI	212	274	348	439	18.23
BMIM TFSI	211	265	340	439	18.20
HMIM TFSI	211	264	339	438	18.18

comparison to the others is due to the higher stability of pure EMIM TFSI. The thermal stability decrease with increasing number of carbon atoms in the alkyl chain from methyl to BMIM TFSI, after which no noticeable change in the decomposition temperature (T_d) can be seen.[28]

Effect of the ILs on Morphology

Layered double hydroxide (Figure 7a,b) is characterized by a layered structure and hexagonal shaped particles with lateral dimensions of 50 - 400 nm. We found that the incorporation of a TFSI-based ionic liquid can improve the filler dispersion throughout the rubber matrix.

The composite containing hydrophobic TFSI-based imidazolium ILs (Figure 7d) exhibited improved filler distribution throughout the elastomer matrix compared with the reference sample (Figure 7c) in which agglomeration within 5 μm was observed. All TFSI-based ionic liquids exhibited good miscibility with the XNBR matrix. The distribution of the TFSI-based ionic liquid in the XNBR/LDH composite was observed via scanning electron microscopy (SEM)combined with energy dispersive

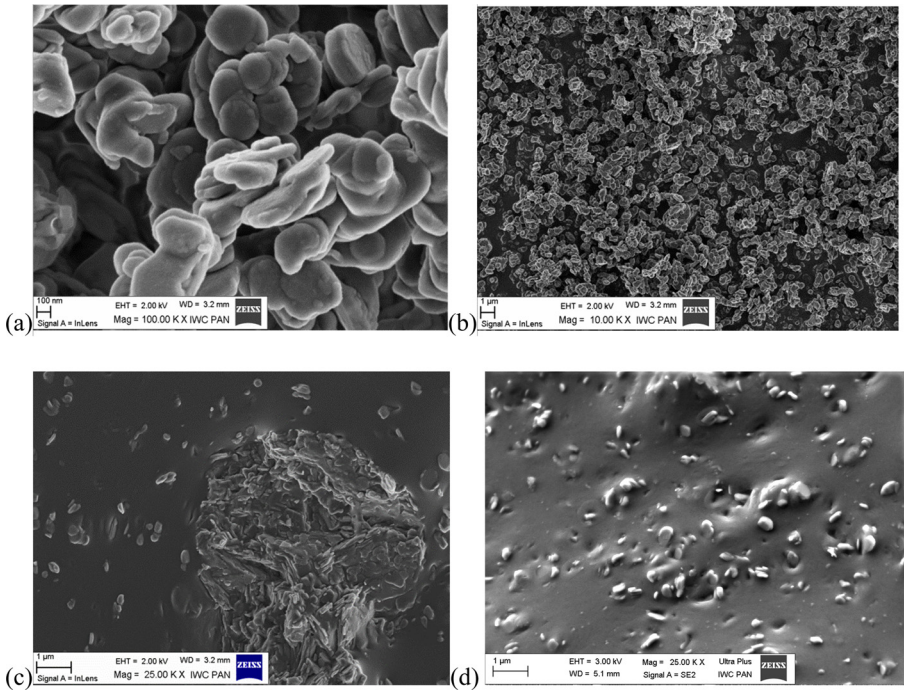

Figure 7.
SEM images of (a, b) LDH particles, (c) XNBR/LDH composite (control sample), (d) XNBR/LDH/BMIM TFSI 15 phr composite.

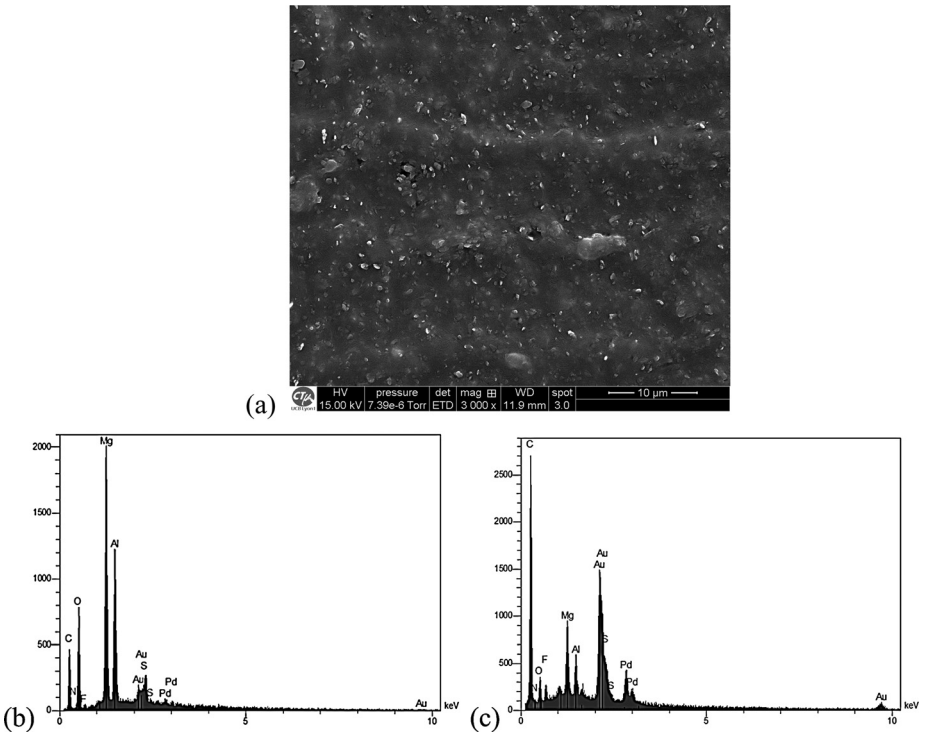

Figure 8.
SEM-EDS mapping of (a) XNBR/LDH/BMIM TFSI 15 phr composite, (b) "filler point", (c) "matrix point".

spectrometry(EDS). The SEM-EDS micrographs of the XNBR/HT containing 15 phr BMIM TFSI are provided in Figure 8(a–c). A higher imidazolium salt concentration (reflected in the intensity of the signal originating from the sulfur and fluorine) was detected in the XNBR matrix (Figure 8c) than at that so-called "filler point" (Figure 8b), which confirms good compatibility between the hydrophobic TFSI IL and the carboxylated rubber.

The effect of 15 phr BMIM TFSI on the XNBR/LDH composite microstructure was also investigated via XRD and the results are presented in Figure 9. The XRD analysis showed the basal reflections (003), (006), (012) and so forth, observed in the crystalline structure of the pure LDH with a 0.76 nm basal spacing (d-value). For the XNBR/LDH and XNBR/LDH/BMIM TFSI composites the positions of the 2θ values remained unchanged from those of the pristine LDH. TheLDH particles used herein at the substantialconcentration of 30 phr, are rather dispersed as aggregates in rubber matrix,also in the presence of 15 phr BMIM TFSI. The intensities of the reflection peaks for the composite containing IL arebelow those of the control sample, which may be explained through the dilution effect of crystalline phase (30 phr LDH

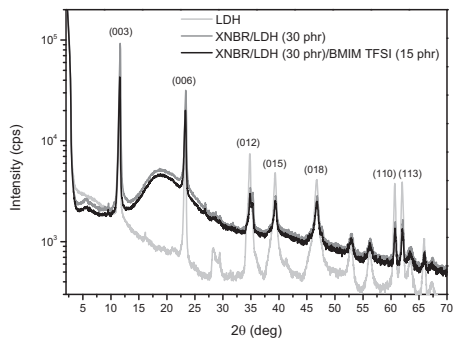

Figure 9.
XRD patterns of pristine LDH and XNBR composites.

and 15 phr BMIM TFSI) or may result from the orientation of the LDH particles in the rubber matrix under the influence of the ionic liquid.

Conclusion

This study examined the relationship between the length of the cation alkyl chain in a TFSI-based IL and the improved ionic conductivity of the XNBR/IL-LDH composite. As indicated, the TFSI-based imidazolium salts act as plasticizers in the rubber matrix and contribute to the reduction in the T_g of the composites. The 1-hexyl-methylimidazolium bis(trifluoromethylsulfonyl) imide (HMIM TFSI) exhibits the highest plasticizing effect in the XNBR/LDH material and the most efficiently increases the ionic conductivity of the composite. The increased motion in the rubber chain segments and lowered viscosity improve the conductivity. However, the impact of the cation alkyl chain length on this parameter was found to be less significant than it could be anticipated. Therefore, compared with HMIM TFSI, the use of EMIM TFSI (or BMIM TFSI) in rubber composition is more preferable considering both mechanical characteristics and ionic conductivity of the resulting composites.

Acknowledgments: The authors wish to acknowledge the Center of Electronic Microscopy of UCB Lyon 1 (Thierry Tamet& Pierre Alcouffe) for performing electronic microscopy analysis.

[1] J. G. Huddleston, A. E. Visser, W. M. Reichert, H. D. Willauer, G. A. Broker, R. D. Rogers, *Green Chem.* **2001**, *3*, 156.
[2] B. Weyershausen, K. Lehmann, *Green. Chem.* **2005**, *7*, 15.
[3] M. D. Bermudez, A. E. Jimenez, J. Sanes, F. J. Carrion, *Macromolecules* **2009**, *14*, 2888.
[4] Y. Lei, Z. Tang, L. Zhu, B. Guo, D. Jia, *Polymer* **2011**, *52*, 1337.
[5] J. Pernak, F. Walkiewicz, M. Maciejewska, M. Zaborski, *Ind. Eng. Chem. Res.* **2010**, *49*, 5012.
[6] E. Marwanta, T. Mizumo, H. Ohno, *Solid State Ionics* **2007**, *178*, 227.
[7] A. A. M. Beigi, M. Abdouss, M. Yousefi, S. M. Pourmortazavi, A. Vahid, *J. Mol. Liq.* **2013**, *177*, 361.
[8] B. D. Fitchett, J. B. Rollins, J. C. Conboy, *J. Electrochem. Soc.* **2005**, *152*, E251.
[9] B. Likozar, *Soft. Matter.* **2011**, *7*, 970.
[10] K. Subramaniam, A. Das, G. Heinrich, *Comp. Sci. Technol.* **2011**, *71*, 1441.
[11] K. Subramaniam, A. das, L. Haussler, C. Harnish, K. W. Stockelhuber, G. Heinrich, *Polym. Degrad. Stab.* **2012**, *97*, 776.
[12] K. Subramaniam, A. Das, D. Steinhauser, M. Kluppel, G. Heinrich, *Eur. Polym. J.* **2011**, *47*, 2234.
[13] D. Steinhauser, K. Subramaniam, A. Das, G. Heinrich, M. Kluppel, *Express Polym. Lett.* **2012**, *11*, 927.
[14] K. Subramaniam, A. Das, G. Heinrich, *Compos. Sci. Technol.* **2013**, *74*, 14.
[15] H. H. Le, X. T. Hoang, A. Das, U. Gohs, K. W. Stoeckelhuber, R. Boldt, G. Heinrich, R. Adhikari, H. J. Radush, *Carbon* **2012**, *50*, 4543.
[16] M. Cho, H. Seo, J. Nam, H. Choi, J. Koo, Y. Lee, *Sens. Actuators, B* **2007**, *128*, 70.
[17] E. Marwanta, T. Mizumo, N. Nakamura, H. Ohno, *Polymer* **2005**, *46*, 3795.
[18] A. Laskowska, A. Marzec, G. Boiteux, M. Zaborski, O. Gain, A. Serghei, *Polym. Int.* **2013**, *62*, 1575.
[19] A. Marzec, A. Laskowska, G. Boiteux, M. Zaborski, O. Gain, A. Serghei, *Eur. Polym. J.* **2014**, *53*, 139.
[20] K. Subramaniam, A. Das, F. Simon, G. Heinrich, *Eur. Polym. J.* **2013**, *49*, 345.
[21] H. Kreyenschulte, S. Richter, T. Gotze, D. Fischer, D. Steinhauser, M. Kluppel, G. Heinrich, *Carbon* **2012**, *50*, 3649.
[22] P. J. Flory, J. Rehner, *J. Chem. Phys.* **1943**, *11*, 521.
[23] A. Laskowska, M. Zaborski, G. Boiteux, O. Gain, A. Marzec, W. Maniukiewicz, *Express Polym. Lett.* **2014**, *8*, 374.
[24] F. R. Costa, S. Pradhan, U. Wagenknecht, A. K. Bhowmick, G. Heinrich, *J. Polym. Sci.* **2010**, *48*, 2302.
[25] D. Basu, A. Das, K. W. Stockelhuber, U. Wagenknecht, G. Heinrich, *Prog. Polym. Sci.* **2014**, *39*, 594.
[26] A. Das, D. Y. Wang, K. W. Stockelhuber, R. Jurk, J. Fritzsche, M. Kluppel, G. Heinrich, *Adv. Polym. Sci.* **2011**, *239*, 85.
[27] L. Ibarra, M. Alzorriz, *J. Appl. Sci.* **2007**, *103*, 1894.
[28] M. Watanabe, H. Tokuda, K. Hayamizu, K. K. Ishii, A. B. H. Susan, *J. Phys. Chem. B* **2005**, *109*, 6103.

